The behavior of CO phases on Rh(110) under static pressures

Cite as: Journal of Vacuum Science & Technology A **8**, 2543 (1990); https://doi.org/10.1116/1.576732
Submitted: 31 August 1989 . Accepted: 25 September 1989 . Published Online: 04 June 1998

J. J. Weimer, J. Loboda-Cackovic, and J. H. Block

The behavior of CO phases on Rh(110) under static pressures

J. J. Weimer, J. Loboda-Cackovic, and J. H. Block
Fritz-Haber-Institut der Max-Planck-Gesellschaft Berlin-Dahlem, Federal Republic of Germany

(Received 31 August 1989; accepted 25 September 1989)

The behavior of CO phases on Rh(110) has been determined under static CO pressures. Three ordered phases are observed as a function of decreasing temperature under equilibrium conditions. Starting from a disordered phase, these are in sequence a $c(2\times2)$, a "(4×2)", and a $(2\times1)p2mg$. In addition, a "(5×2)" phase forms irreversibly just prior to the $(2\times1)p2mg$ on cooling in low CO pressures (less than 10^{-5} Pa). Formation of the $(2\times1)p2mg$ phase is found to be activated, which may indicate that surface reconstruction is involved.

I. INTRODUCTION

The study of various phases of CO on transition-metal surfaces has received renewed interest in the past years. In regard to low-energy electron diffraction (LEED) studies of CO on the [110] surfaces of Rh,[1,2] Pd,[3,4] Pt,[5-7] Ni,[8,9] and Ir,[10] a common characteristic is that the final equilibrium phase at saturated CO coverage ($\Theta_{CO}=1$) is found to be mainly if not exclusively a $(2\times1)p2mg$ phase. Recent LEED investigations of this phase on Pd(110) have shown that its formation is activated,[4] and a surface reconstruction was proposed as the cause. This proposition has even more recently also been advanced in a reinterpretation of infrared results from CO on Pd(110).[11,12]

The objective of this report is to present results of a detailed study of the behavior of and phase diagram for CO on the Rh(110) under static CO pressures. A previous investigation of the $(2\times1)p2mg$ CO phase on Rh(110)[1] was the first to point out that this phase is common to the [110] faces of the above metals. Our work has determined that this similarity extends further for Pd and Rh, in that formation of the $(2\times1)p2mg$ CO phase is activated on both. Our investigations also show a more extensive phase diagram than had been reported.[1,2] A separate publication will deal with the details of the LEED patterns and overlayer structures for the phases as a function of Θ_{CO} and temperature.[13]

II. EXPERIMENTAL DETAILS

A detailed description of the apparatus and vacuum chamber has been given elsewhere.[14] Further modifications have since replaced diffusion pumps on the gas inlet and differentially pumped mass spectrometer with turbomolecular pumps. The base pressure in the chamber is typically 1×10^{-8} Pa or lower during experiments.

The LEED facilities used have been discussed in detail previously.[14] A video camera mounted on a window viewport opposite the screen records the LEED pattern, and line profiles within a given window are extracted by a computer system for video-LEED analysis also described elsewhere.[14,15] The suppressor voltage to the LEED screen and the dc heating current to the crystal are chopped in synchronization with the video frame rate and data recorded during the off-cycle of the heating current to avoid aberations caused by the magnetic field induced by the heating current on the LEED pattern.

The Rh(110) crystal had been prepared by standard methods and was used extensively in previous LEED work on hydrogen structures,[16] which assured that it was largely clean of bulk impurities. Cleaning of the sample after bakeout of the vacuum chamber consisted of an Ar ion sputter for a few hours at 750 eV with the sample at about 1100 K, followed by a brief (15 min) oxygen treatment ($P\sim5\times10^{-5}$ Pa) at the same temperature to remove carbon and a longer (30–45 min) hydrogen treatment ($P\sim7\times10^{-5}$ Pa) at about 700 K (to remove possible subsurface oxygen). The surface was then annealed 5 min or less at about 1290 K.

In any event of uncertainty, the surface cleanliness and order was checked by observing the sequence of hydrogen LEED patterns that occur on Rh(110), as they have been found to be extremely sensitive to impurities on the surface.[16] This was confirmed during the course of our work, as unsharp hydrogen induced LEED patterns *always* indicated trace impurities on the surface (generally silicon or carbon). Following a brief ($\sim$30 min) sputter and oxygen–hydrogen-anneal sequence, the surface could be returned to a clean state if silicon was involved. Otherwise a brief oxygen–hydrogen-anneal sequence was used to remove carbon.

III. RESULTS

Five ordered overlayer structures are observed for CO/Rh(110) as a function of Θ_{CO} during dosing below room temperature,[13] of which four are relevant to the results observed in static CO. At low coverages, $\Theta_{CO}<\sim0.25$, no overlayer LEED stuctures are seen, indicating a disordered, two-dimensional (2D) gas region. A $c(2\times2)$ phase appears at $\Theta_{CO}\sim0.50$, followed at $\Theta_{CO}\sim0.75$ by a (4×2) phase. The CO induced LEED spots for this phase are extremely faint and very diffuse, making a determination of the exact space group within (4×2) difficult [$p(4\times2)$ or $c(4\times2)$ for example]. The (4×2) structure is followed almost immediately by a somewhat more intense but equally diffuse LEED pattern indicating a phase of possible (5×2) symmetry. The pattern is similar to that reported as $c(5/4\times2)$ for CO on Cu(110).[17] Beyond $\Theta_{CO}\sim0.85$ (depending on temperature), additional LEED spots for a $(2\times1)p2mg$ CO phase also appear and grow in intensity at the expense of the (5×2) CO phases spots with increasing Θ_{CO}. The (5×2) phase exists as a pure phase above (in temperature) the

 0734-2101/90/032543-05$01.00

mixed phase region at $\Theta_{CO} \sim 0.9$. The final LEED pattern at $\Theta_{CO} = 1.0$ is a sharp, intense $(2\times1)p2mg$ pattern reported earlier on Rh(110) from room-temperature adsorption studies.[1,2] These earlier studies of the $(2\times1)p2mg$ CO structure first classified it as $(2\times1)p1g1$ because the presence of a glide plane axis explained missing $(\pm\frac{1}{2}\,h,0)$ order spots, however a later analysis considered the presence of a mirror plane and classified the space group as $(2\times1)p2mg$.[18] We will refer to this structure simply as (2×1) in what follows.

The phase diagram under static CO pressure is shown in Fig. 1. The existence regions for the four previously mentioned phases and the disordered region are illustrated. With the exception of the (5×2), the phases could be reached reversibly on heating or cooling at constant pressure or by increasing or decreasing CO pressure at constant temperature. The measured points on the phase boundaries were determined in two separate experiments for transitions to and from the (2×1) phase and to and from the (4×2) phase, respectively. In each experiment, line profiles were measured on the appropriate CO overlayer spot as a function of temperature at a particular CO pressure during heating and, immediately following, during cooling through the transition region. The square root of peak intensity corrected for a linear background was plotted as a function of temperature and the critical temperatures of the transitions determined from the inflection points of the curves. In the case of the (2×1) transitions, profiles were measured in both [01] and [10] at 47 eV. For the (4×2) transitions, additional profiles were measured on the (5×2) and (2×1) phase spots as a control for comparison between the two experiments. At the primary beam energy where the $(\frac{3}{4},\frac{1}{2})$ spots for the (4×2) phases were measured (58 eV), the $(\frac{1}{2}, 1)$ spots for the (2×1) were less intense then optimum. A qualitative comparison between the two experiments showed that the trends in the (2×1) phase critical temperatures were reproduced.

The boundaries are denoted as "equilibrium" when the two opposing phases where reached reversibly, although the exact boundary position varied with direction. This observed hysteresis of the boundary position would not be seen on true equilibrium diagram, to the extent that the phase boundaries would be single isosteres, as for example in the work for CO/Pd(100)[19] or CO/Pd(110).[14] Due to kinetic effects, the transitions observed in this work do not occur at the same temperature, even for the slow (but not infinitely slow) heating or cooling rate used, and a transition region is therefore obtained.

Transitions curves and phase regions obtained from the (4×2) and concurrently measured (2×1) spots are shown in Fig. 2 for heating and cooling at 8×10^{-6} Pa. The transition temperature into the (5×2) was taken from that for the disappearence of the (4×2) on cooling, as the (5×2) spots proved too broad in the [01] direction of the window to establish a definite transition point in most cases. Transition curves for the (2×1) phase are shown in Fig. 3 for heating and cooling at a series of pressures.

In addition to the measured points, a visual observation at one CO pressure (3.8×10^{-5} Pa) of the $c(2\times2)$ phase transition to and from the disordered region and to and from the (4×2) region was made, and the points marking the observed complete disappearence of the $c(2\times2)$ spots in either direction (436 and 486 K) are shown. The transition region for the $c(2\times2)$ to disordered phase shown was obtained by combining results for the Θ_{CO} versus temperature phase diagram[13] and isosteres for coverages $\Theta_{CO} = 0.25$ and

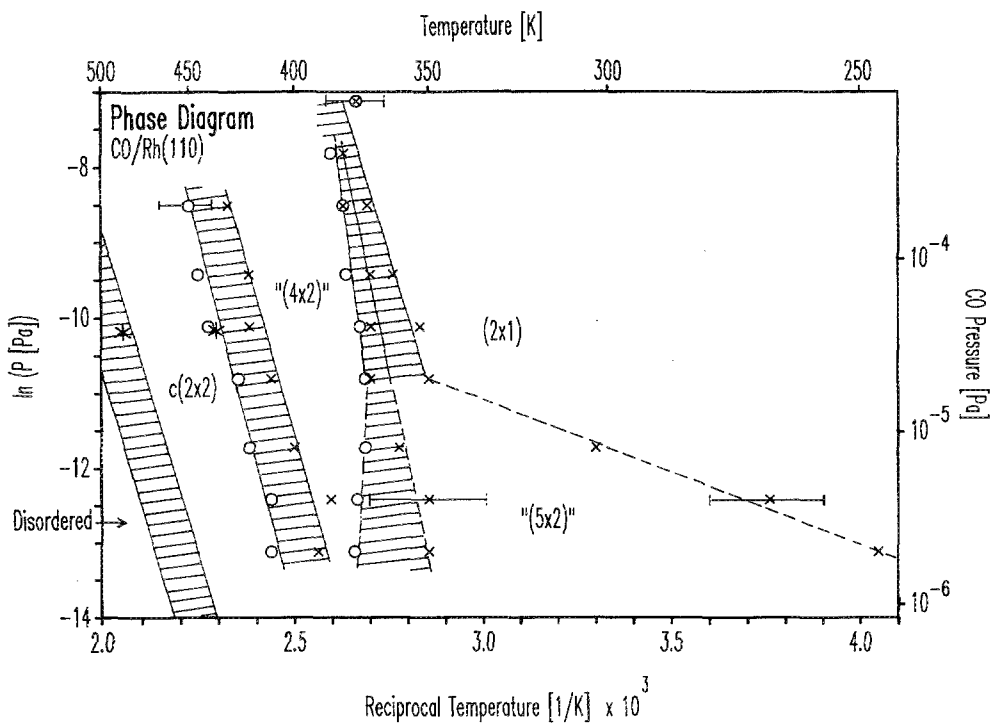

FIG. 1. The phase diagram for CO on Rh(110) under static CO pressures. The existence regions of the various phases are marked by transition regions (striped areas) determined by the critical temperatures of the phases obtained during video-LEED measurements of spot profiles for heating (O) or cooling (×) (0.5 K/s) the sample at the given CO pressure. The additional points (*) show disappearence boundaries of the $c(2\times2)$ phase from visual observations, and the transition region between the $c(2\times2)$ and the disordered phases was determined as described in the text. The significance of the "equilibrium" (—) and non-equilibrium (- - -) boundaries is also discussed in the text.

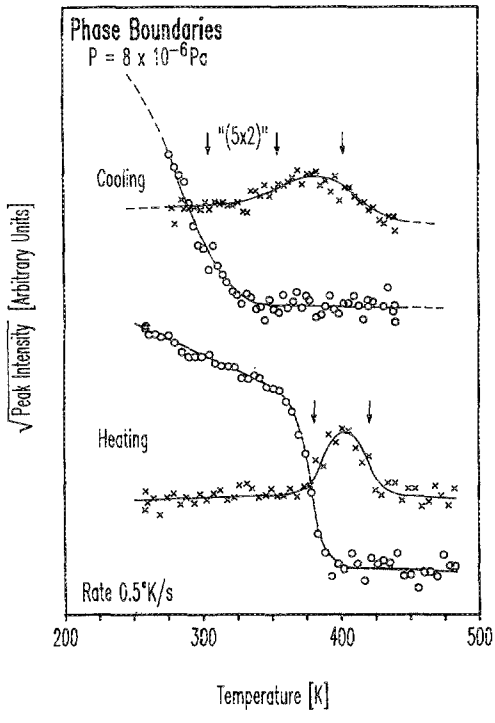

FIG. 2. Square root of peak intensity vs temperature from profiles on spots of the $(2\times1)p2mg$ phase (O) and (4×2) phase ($\times$) during heating or cooling (0.5 K/s) Rh(110) in CO at 8×10^{-6} Pa. The (4×2) curves are multiplied by a factor of 2 over the scale for the (2×1) curves. The transition temperatures are noted approximately with arrows and the existence regions of the (5×2) phase phase labeled. Solid lines are guides through the data.

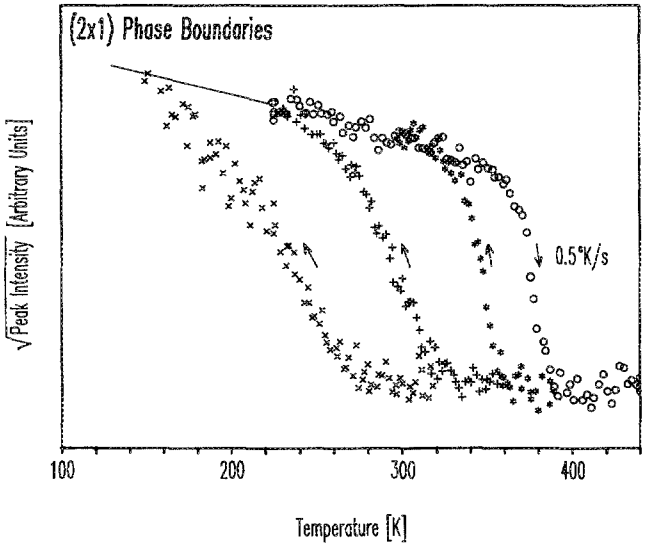

FIG. 3. Square root of peak intensity vs temperature from profiles on the (1/2,1) spot for the $(2\times1)p2mg$ phase during heating or cooling (0.5 K/s) Rh(110) in CO at various pressures. For clarity, only one heating curve (2×10^{-4} Pa) is shown, as those for all other pressures were in essentially the same position. $\times$ (2×10^{-6}), + (8×10^{-6}), * (2×10^{-5} Pa), and O all above.

$\Theta_{CO} = 0.30$ from isobaric measurements of work function changes for CO on Rh(110).[20]

The errors in the measurements of the critical temperatures are a summation of those from the thermocouple accuracy (estimated $\pm$ 2 K) and that from the accuracy of determining the inflection point. The latter was overriding, being as much as $\pm$ 20 K for the broad (4×2) and (5×2) transitions, and representative errors are shown in Fig. 1 on select points. The heating and cooling rates were set as equal at 0.5 K/s, but the cooling rate was sometimes lower (0.3 K/s) for lower temperatures. The absolute accuracy of the CO pressure is estimated as possibly 10%–15% (too low) when accounting for gauge sensitivities and a later calibration against a viscovac spinning ball manometer, however, no correction was made for these factors in Fig. 1.

IV. DISCUSSION

The existence regions for the disordered $c(2\times2)$, (4×2), and (2×1) phases agree with those seen in the Θ_{CO} versus temperature diagram[13] when coverages are compared via isosteres measured separately from work function changes.[20] These three ordered phases are also seen in various stages on select [110] faces of the other face-centered-cubic (fcc) metals, as will be discussed in detail elsewhere.[13] The exact position of the equilibrium (5×2) existence region in static CO is uncertain because this phase is only accessed irreversibly by cooling in low CO pressures ($P < 10^{-5}$ Pa), as shown in Fig. 1 by the broadening of the (5×2) region with decreasing pressure. This behavior indicates that formation of the (2×1) phase from the (5×2) phase is activated.

Further evidence for an activation barrier for the (2×1) phase is seen in Figs. 2 and 3 from changes in the sharpness of the (2×1) transition curves and in Fig. 1 in the width of the neighboring transition region. On heating out of the (2×1) phase, the boundary temperature is sharp (Figs. 2 and 3) and is nearly independent of CO pressure (Θ_{CO} under equilibrium conditions) over four orders of magnitude (Fig. 1). The transition temperatures coincide with the onset of thermal desorption from the phase (373 K), even at pressures down to 10^{-8} Pa and for a much higher heating rate (5 K/s) used in thermal desorption spectroscopy.[13,20] On cooling from the (4×2) for successively lower CO pressures, the onset of the transition requires more time at the successively lower temperatures where $\Theta_{CO} \sim 1$ (for equilibrium adsorption/desorption). The transition regions next to the (2×1) phase therefore appear to broaden on the low-temperature (cooling) side (Fig. 1). Correspondingly, the (2×1) transition boundary is not as sharp on cooling as on heating (Figs. 2 and 3). This latter effect was evident at all pressures measured, even when the critical temperatures on heating and cooling where nearly identical.

The behavior of the (2×1) CO phase on Rh(110) is similar to that found on Pd(110)[4]; on both metals, the transition into or out of the phase is activated, and the LEED spots from the phase are sharper and more intense than those expected from a CO overlayer structure alone.[21] The spots for the $c(2\times2)$, (4×2), and (5×2) phases for example

showed essentially no intensity above about 120 eV, while those for the (2×1) remained as intense as the Rh(110) substrate spots even up to 500 eV or above. The cause of this unusual behavior for (2×1) CO on Pd(110) was proposed to be a reconstruction of the substrate lattice.[4] Recent analysis from an infrared spectroscopic study indeed proposes significant substrate reconstruction on Pd(110) in the CO phase forming prior to the (2×1) *p2mg*.[12]

A reconstruction of the Rh(110) surface on formation of the CO (2×1) phase would similarly explain the results of this work.[13] This proposition must await confirmation from analysis with methods more sensitive to the specific nature of a reconstruction or a thorough structure calculation considering possible reconstruction models for LEED intensity versus energy measurements. Differences are apparent in the overall phase and thermal desorption behavior of CO on Rh(110)[13,20] as compared to Pd(110),[4] and other adequate models of the (2×1) CO phase have been found, for example as from a LEED *R*-factor analysis for CO on Ni(110)[9] or an angle-resolved photoelectron spectroscopic study of the same system[22] (although only the tilt angle of the CO was of concern in both cases, and specific consideration of substrate reconstruction was not made). An independent investigation of the vibrational spectroscopic properties of adsorbed CO on Rh(110) is in progress,[23] which might clarify the question of the role of a possible surface reconstruction.

The transition region between (4×2) and $c(2\times2)$ phases is at $\Theta\sim0.7$ when considering isosteres determined by work-function changes,[20] which agrees with the onset of the transition during dosing at low temperatures (80 K).[13] The extrapolated position of the $c(2\times2)\leftrightarrow$disordered phase transition region in Fig. 1 is also confirmed by the visual observation on the $c(2\times2)$ phase spots. Whether the (5×2) phase truly exists in a narrow equilibrium region between the (4×2) and (2×1) phases, as implied in Fig. 1 from the points of the two separate cooling experiments (and expected at $\Theta\sim0.9$),[13] could not be determined with certainty.

Under equilibrium conditions and with the assumption that the transition boundaries mark isosteres in the pressure versus temperature phase diagram, the slope of the transition line is equal to the adsorption enthalpy, ΔH_{ads}.[19] The values for the various "equilibrium" transitions are given in Table I. The high value during the $(2\times1)\rightarrow(4\times2)$ transition (309 kJ/mol) shows the effects of the activation barrier. Note that inclusion of the point at 8×10^{-4} Pa (375 K) in the least-squares fit for ΔH_{ad} during the transition $(2\times1)\rightarrow(4\times2)$ gave a much higher value (approaching infinity). Within the error limits, the transition at 8×10^{-4} Pa occurred at a noticeably lower temperature than the transitions at somewhat lower pressures. A lower position (in temperature) of the actual $(2\times1)\rightarrow(4\times2)$ boundary (for example, at that for the cooling measurements) and an opening of an equilibrium (5×2) region at higher pressures might be the cause. The values determined during cooling through the transitions $(4\times2)\rightarrow(5\times2)$ and (4×2) or $(5\times2)\rightarrow(2\times1)$ may be more representative of ΔH_{ads} at the transition Θ_{CO} in this respect.

TABLE I. Adsorption enthalpies, ΔH_{ads}, calculated from the "equilibrium" boundaries shown in Fig. 1.

Transition	Value (kJ/mol)
$(2\times1)\rightarrow(4\times2)$	309 ± 40
$(5\times2)\rightarrow(2\times1)$	109 ± 21
$(4\times2)\rightarrow(5\times2)$	153 ± 20
$(4\times2)\rightarrow c(2\times2)$	150 ± 15
$c(2\times2)\rightarrow(4\times2)$	130 ± 15

V. CONCLUSIONS

The behavior of CO phases on Rh(110) has been determined as a function of CO pressure and sample temperature. Three ordered equilibrium phases are observed, a $c(2\times2)$ phase at $\Theta_{CO}\sim0.5$, a (4×2) phase at $\Theta_{CO}\sim0.75$, and a $(2\times1)p2mg$ phase at $\Theta_{CO}=1.0$. In addition, a (5×2) phase is seen under irreversible conditions when the sample is cooled in low pressures ($P>10^{-5}$ Pa) of CO. The irreversibility during the transitions associated with the (2×1) phase and the abruptness of the transition out of the (2×1) phase compared to the transition into the phase lead to the conclusion that its formation is activated. A reconstruction of the Rh(110) would explain this conclusion and further investigations are warranted to confirm this proposition.

ACKNOWLEDGMENTS

The authors are grateful for the informative discussions with Professor K. Christmann and for his loan of the Rh(110) crystal during this work and to M. Ehsasi for providing results of isosteric heat measurements prior to publication. One of us (J. J. W.) acknowledges a stipend from the Max-Planck-Gesellschaft. This work was supported by the Deutsche Forschungsgemeinschaft (SFB 6/81).

[1] R. A. Marbrow and R. M. Lambert, Surf. Sci. **67**, 489 (1977).
[2] R. J. Baird, R. C. Ku, and P. Wynblatt, Surf. Sci. **97**, 346 (1980).
[3] M. A. Chesters, G. S. McDougall, M. E. Pemble, and N. Sheppard, Surf. Sci. **164**, 425 (1985).
[4] J.-W. He and P. R. Norton, J. Chem. Phys. **89**, 1170 (1988).
[5] P. Hofmann, S. R. Bare, and D. A. King, Surf. Sci. **117**, 245 (1982).
[6] W. N. Unertl, T. E. Jackman, P. R. Norton, D. P. Jackson, and J. A. Davies, J. Vac. Sci. Technol. **20**, 607 (1982).
[7] T. E. Jackman, J. A. Davies, D. P. Jackson, W. N. Unertl, and P. R. Norton, Surf. Sci. **120**, 389 (1982).
[8] R. J. Behm, G. Ertl, and V. Penka, Surf. Sci. **160**, 387 (1985).
[9] D. J. Hannaman and M. A. Passler, Surf. Sci. **203**, 449 (1988).
[10] K. Christmann and G. Ertl, Z. Naturforsch. Teil A **28**, 1144 (1973).
[11] R. Raval, M. A. Harrison, and D. A. King, Surf. Sci. **211/212**, 61 (1989).
[12] R. Raval, S. Haq, M. A. Harrison, G. Blyholder, and D. A. King, Chem. Phys. Lett. (submitted).
[13] J. J. Weimer, J. Loboda-Cackovic, and J. H. Block, J. Chem. Phys. (to be published).
[14] J. Goschnik, M. Wolf, M. Grunze, W. N. Unertl, J. H. Block, and J. Loboda-Cackovic, Surf. Sci. **178**, 831 (1986).
[15] K. Müller, Ber. Bunsenges. Phys. Chem. **90**, 184 (1986).

[16] K. Christmann, M. Ehsasi, W. Hirschwald, and J. H. Block, Chem. Phys. Lett. **131**, 192 (1986); M. Ehsasi (private communication).
[17] C. Harendt, J. Goschnick, and W. Hirschwald, Surf. Sci. **152/153**, 453 (1985).
[18] M. Nishijima, S. Masuda, Y. Sakisaka, and M. Onchi, Surf. Sci. **107**, 31 (1981).
[19] J. C. Tracy and P. W. Palmberg, J. Chem. Phys. **51**, 4852 (1969).
[20] M. Ehsasi, K. Christmann, and J. H. Block (to be published); M. Ehsasi (private communication).
[21] M. Fink, M. R. Martin, and G. A. Somarjai, Surf. Sci. **29**, 303 (1972).
[22] H. Kuhlenbeck, M. Neumann, and H.-J. Freund, Surf. Sci. **173**, 194 (1986).
[23] K. Christmann (private communication).